

A Linear Cochlear Model with Active Bi-directional Coupling

Bo Wen and Kwabena Boahen

Department of Bioengineering, University of Pennsylvania, PA, USA

Abstract—We present a linear active cochlear model that includes the outer hair cell (OHC) forces, which are delivered onto upstream and downstream basilar membrane (BM) segments through Deiters’ cells (DCs) and their phalangeal processes (PhPs). Due to the longitudinal tilt of the OHC towards the base and the oblique orientation of the PhP towards the apex, each BM segment receives both feed-forward and feed-backward OHC forces. Transverse BM fibers are actively coupled longitudinally through these bi-directional OHC forces, included in a cochlear model for the first time. We present simulation results that demonstrate large amplification and sharp tuning, and we analyze the underlying mechanism.

Keywords—Outer hair cell, phalangeal process

I. MODELING EFFORTS ON ACTIVE AMPLIFICATION

As the main vibrating organ within the cochlea, the basilar membrane (BM) is composed of transverse fibers that are only weakly coupled longitudinally. From the base to the apex, the BM fibers increase in width and decrease in thickness. The resulting exponential decrease in stiffness gives rise to the passive frequency tuning of the cochlea. The outer hair cells (OHCs) inside the organ of Corti (OC) are thought to amplify BM motion, as they actively change their length when stimulated electrically [1]. This active amplification results in exquisite sensitivity, high frequency selectivity, and high-sound-level compression.

A number of modelers have added OHC electro-motility to passive cochlear models to account for the active amplification [2-6]. These models differ in how the OHCs exert forces on the BM, and in the role of other structures within the cochlear partition (CP). A few recently developed active cochlear models take into account the OHCs’ basal tilt [5-8]. These models hypothesized, counter-intuitively, that this tilt amplifies BM motion and sharpens its tuning through “feed-forward forces” that act on downstream BM segments.

We propose a linear active model that produces realistic cochlear responses based on a novel interpretation of OHC motility. Similar to the feed-forward models, our model takes OHC tilt into account. Equally important in our model, however, is the oblique orientation of the phalangeal process (PhP), which we also take into account. Through the PhP, the OHC force can be transmitted backward onto upstream BM segments. Therefore, the OHC force is exerted on the Deiters’ cell (DC) sitting on one BM segment, either directly by the OHC or indirectly through the PhP, with opposing effects. These feed-forward and feed-backward forces introduce active bi-directional longitudinal coupling between BM segments.

II. ACTIVE BI-DIRECTIONAL COUPLING

Our model hypothesizes that the triangular mechanical unit plays an active role in amplifying BM responses, which is formed by an OHC, the PhP of the DC on which the OHC sits, and the portion of the reticular lamina (RL) between the stereocilia end of the OHC and the apical tip of the PhP.

Fig. 1 shows the arrangement of OHCs in the CP (derived from [9, 10]), which divides into a number of segments from the base to the apex. Each segment includes one DC sitting on the BM, the apical tip of one PhP and the stereocilia end of one OHC, both attached to the RL segment. Approximating the anatomy, we assume that when the stereocilia end of an OHC lies in the segment $i-1$, its basolateral end lies in the immediately apical segment i . Furthermore, the DC in segment i sends a PhP that angles toward the apex of the cochlea, with its apical end inserted just behind the stereocilia end of the OHC in segment $i+1$.

In the case of rigid OHCs (without motility), each BM segment moves up and down as the pressure difference between the fluids in the scala vestibuli (SV) and the scala tympani (ST) acts on the BM. Fig. 1B depicts a transverse view of the CP, which reveals a critical structure called

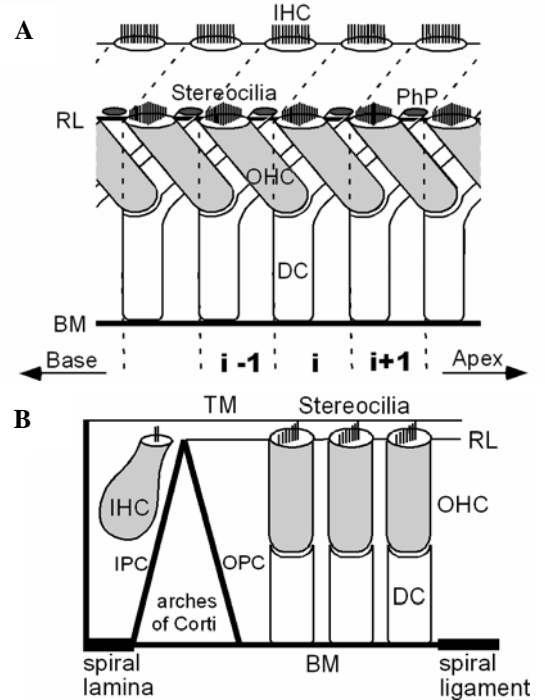


Fig. 1. Microanatomy of the cochlear partition (CP). (A) Longitudinal view. Only the outermost row of outer hair cells is shown. Three CP segments are labeled (i.e., $i-1$, i , and $i+1$). (B) Transverse view. The tectorial membrane (TM) is not shown in A.

arches of Corti. The arches of Corti is formed by the inner pillar cell (IPC), the outer pillar cell (OPC) and part of the BM transverse fiber. The base of the OPC works as a rigid pivot point when the BM fiber vibrates up and down [11]. Given this microanatomy, the movement of the BM causes the stereocilia in the same segment to deflect due to the radial shear motion between the tectorial membrane (TM) and the RL.

In the case of OHCs with motility, the deflection of stereocilia in turn results in the contraction or expansion of the OHC because their defelection causes ions to flow across the OHC's membrane, resulting in depolarization or hyperpolarization of the OHC. Due to its longitudinal basal tilt, the OHC in segment $i-1$ exerts a force on the BM that sits in the downstream segment i (through the DC), thereby the BM is pulled to or pushed away from the RL. Thus, the vibration of BM segment i is enhanced by the displacement of the upstream segment, $i-1$.

In segment $i+1$ of the CP, the deflection of stereocilia due to the upward or downward displacement of the BM causes the OHC whose stereocilia end lies in the segment $i+1$ to contract or expand, thus pulling down or pushing up the RL to some extent (meanwhile, BM segment $i+2$ is pulled up or pushed down due to the feed-forward mechanism). The driven RL segment $i+1$ then pushes down or pulls up the rigid PhP and the whole DC, exerting a force on the BM segment i . Thus, the vibration of BM segment i is, additionally, opposed by the displacement of the upstream segment, $i+1$.

In this way, OHC motility and the microanatomy of the CP give rise to feed-forward and feed-backward forces that introduce active bi-directional longitudinal coupling between BM segments. Hence, each BM segment receives, and sends, coupling forces from, and to, its upstream and downstream segments. The motion of BM segment $i-1$ reinforces that of segment i while the motion of segment $i+1$ opposes that of segment i .

III. THE 2D LINEAR ACTIVE MODEL

For the cochlear fluid motion, we define a velocity potential, $\phi(x, y, t)$, which, due to its incompressibility, satisfies Laplace's equation: $\nabla^2 \phi = 0$, where ∇^2 is the laplacian operator. This potential is related to fluid velocities in the x and y directions:

$$V_x = -\partial\phi/\partial x \quad \text{and} \quad V_y = -\partial\phi/\partial y.$$

These velocities, V_x and V_y , match the stapes motion ($\partial\phi/\partial x = f(t)$ at $x = 0$), go to zero at the bottom and apical walls ($\partial\phi/\partial y = 0$ at $y = 0$, and $\partial\phi/\partial x = 0$ at $x = L$), and match the BM motion in the middle ($-\partial\phi/\partial y = \partial\delta/\partial t$ at $y = h$). Here, δ is the BM displacement and $f(t)$ is the stapes velocity (inward positive).

According to the Newton's second law, the BM's vertical motion (downward positive) can be described as follows.

$$P_d + F_{\text{OHC}} = S(x)\delta + \beta(x)\partial\delta/\partial t + M(x)\partial^2\delta/\partial t^2,$$

$$F_{\text{OHC}} = \alpha S(x)(\gamma\delta(x-d) - \delta(x+d)),$$

where $S(x)$ is its stiffness, $M(x)$ is its mass, and $\beta(x) = \zeta\sqrt{S(x)M(x)}$ is its damping, per unit area. Here, P_d is the difference in fluid pressure between the SV and the ST. F_{OHC} combines feed-forward and feed-backward OHC forces, expressed as a fraction α of the BM stiffness. α denotes the OHC motility factor, which represents the OHC force per unit BM displacement. γ is the ratio of the feed-forward to the feed-backward coupling, representing relative strengths of the OHC forces exerted on the BM segment through the DC, directly, and through the tilted PhP. d denotes the tilt distance, which is the horizontal displacement between the source and the recipient of the OHC force.

As pressure $P = \rho\partial\phi/\partial t$, we have the BM boundary condition:

$$2\rho\partial\phi/\partial t = S(x)\delta + \beta(x)\partial\delta/\partial t + M(x)\partial^2\delta/\partial t^2 + \alpha S(x)(\delta(x+d) - \gamma\delta(x-d)),$$

at $y = h$. The factor 2 accounts for fluid on both sides of the membrane; their motions are complementary because the fluid is incompressible.

IV. SIMULATION RESULTS AND ANALYSIS

First, we present a solution procedure of our model, which yields solutions for the BM's displacement δ and the wavenumber k , following Watts's approach [12]. For both δ and k , we explore the effects of changing the motility factor α . Second, we derive closed-form expressions that relate k to the model parameters.

A. Simulation Results

We assume a solution form for the velocity potential that represents a wave traveling in the $+x$ direction, while satisfying Laplace's equation and the bottom wall boundary condition:

$$\phi(x, y, t) = B \cosh(ky) e^{i(\omega t - kx)},$$

where B is a constant. Based on this guess, the form of δ can be expressed as

$$\delta(x, t) = iB e^{i(\omega t - kx)} k \sinh(kh) / \omega.$$

By substituting these forms and their corresponding derivatives into the BM boundary condition, we derive a dispersion relation, which describes the relation between the wave's energy (i.e., frequency) and its momentum (i.e., wavenumber k) (see Section IV.B). Given any input frequency, we can solve this dispersion relation for k , and hence obtain the BM displacement $\delta(x, t)$.

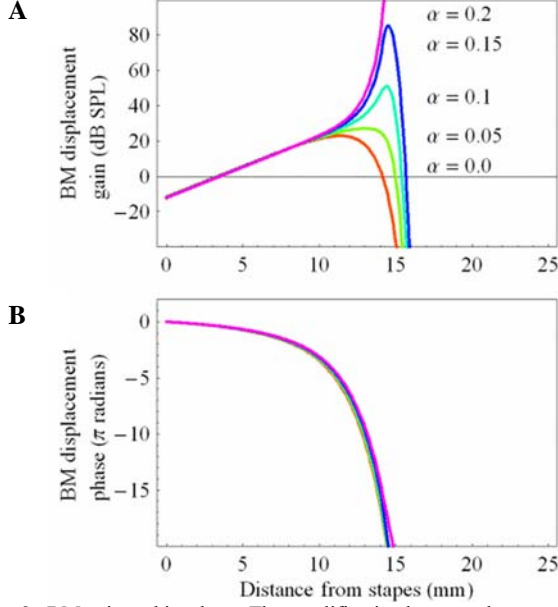


Fig. 2. BM gain and its phase. The amplification becomes larger and the tuning gets sharper as α increases from 0.0 to 0.2.

Fig. 2 shows the amplitude and phase of the BM displacement, normalized by the stapes displacement, for a 2 KHz tone, with the motility factor α varying from 0.0 to 0.2. The model parameters we used in the simulation for both δ and k , which are from the cat cochlea (similar to those used in [5]), are listed in Table I. As α increases from 0.0 to 0.15, gain increases, tuning sharpens, and the characteristic place moves apicalward. Values of Q_{10s} , peak heights, and characteristic places are listed in Table II. When $\alpha = 0.15$, the BM displacement gain amounts to 85 dB; the phase accumulation at the characteristic place is about 10 cycles. When $\alpha = 0.2$, the BM response explodes. We will return to this in Section V.

TABLE I
THE MODEL PARAMETERS

Parameters and denotation	Values	Unit
Cochlear duct height h	1.0	mm
Cochlear duct length L	25.0	mm
Fluid density ρ	$1.0 \cdot 10^{-3}$	g/mm^3
BM mass per unit area $M(x)$	$3.0 \cdot 10^{-5}$	g/mm^2
BM stiffness per unit area $S(x)$	$5.0 \cdot 10^4 e^{-0.4x}$	$\text{g}/(\text{mm}^2 \text{s}^2)$
BM damping ratio ζ	0.2	
Tilt distance d	$7.1 \cdot 10^{-2}$	mm
Segment length Δ	$7.1 \cdot 10^{-2}$	mm
OHC motility factor α	0.0-0.2	
Forward/backward ratio γ	0.3	

TABLE II
SUMMARY OF MODEL RESPONSES

OHC motility factor α	Q_{10}	Peak Amplitude (dB SPL)	Characteristic Place (mm)
0.0	0.56	22.93	11.43
0.05	0.57	27.03	13.07
0.10	2.88	51.03	14.50
0.15	5.44	85.29	14.57

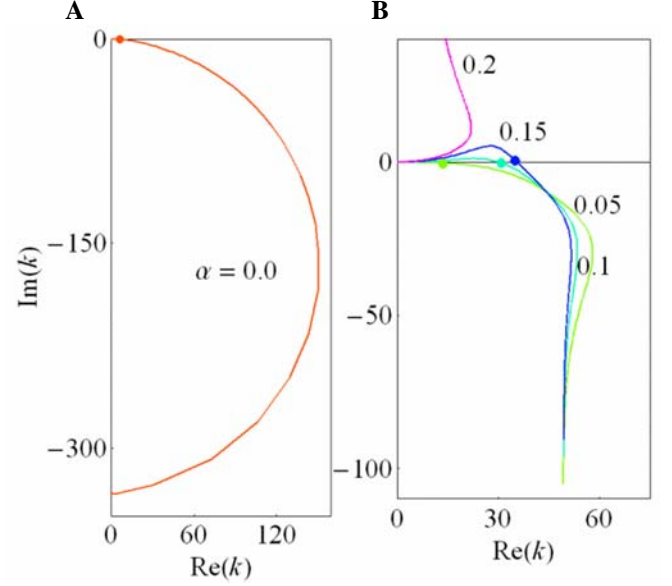


Fig. 3. Wavenumber loci for 2KHz. (A) OHC motility factor $\alpha = 0.0$. (B) $\alpha = 0.05, 0.1, 0.15, \text{ and } 0.2$. The dots mark where the BM displacement peaks.

For wave propagation in the $+x$ direction, the real part of the wavenumber, k_r , is inversely related to the wavelength, whereas the imaginary part, k_i , is related to the wave-amplitude. Thus, wave propagation in the passive and active models may be compared by plotting the real and imaginary parts of the wavenumber. Fig. 3 shows the loci of the wavenumber k when input is a 2KHz tone, with the motility factor α varying from 0.0 to 0.2. As the wave propagates, it transitions from long wave to short wave, where its wavelength becomes much smaller than the cochlear duct's height.

B. Analytical Treatment

We derive approximations that describe three characteristic features of the wave-number locus, particularly for the active case (i.e., $\alpha > 0$). First, why does it enter the first quadrant? Second, what is the asymptotic value of the real part? And, third, when is the imaginary part equal to zero? The first question sheds light on how active amplification arises. The second addresses why the wavelength remains short in the cut-off region, unlike the passive case. And the third reveals how the characteristic place depends on the model's parameters.

Setting the forward to backward ratio $\gamma = 1$ ($\gamma = 0.3$ used for above simulations) as an approximation, we obtain a dispersion relation of the form:

$$\frac{k \tanh(kh)}{1 + i\alpha S(x)k \tanh(kh) \sin(kd) / \rho\omega^2} = \frac{2\rho\omega^2}{S(x) + i\omega\beta(x) - \omega^2 M(x)}$$

In the short-wave region, $\tanh(kh) \approx 1$. Substituting this approximation yields

$$2\alpha k \sin(kd) - (\zeta\Omega + i(\Omega^2 - 1))k - 2i(\rho / M(x))\Omega = 0,$$

where $\Omega = \omega/\omega_n$ and $\omega_n(x) = \sqrt{S(x)/M(x)}$. As $\sin(kd) \approx kd$ when $|kd| \ll 1$, we have

$$2\alpha dk^2 - (\zeta\Omega + i(\Omega^2 - 1))k - 2i(\rho/M(x))\Omega = 0.$$

Near the base, the input frequency is much lower than ω_n , so $\Omega^2 \ll 1$. And we can assume that $\zeta\Omega \ll 1$ as well. Hence, we find that

$$k = (\sqrt{i16\alpha(\rho d/M(x))\Omega - 1 - i})/4\alpha d.$$

Ω increases as the wave propagates, due to the decrease in ω_n . Thus, the first term pushes the wavenumber into the first quadrant if $\alpha > 0$. Therefore, a non-zero OHC motility factor is the source of active amplification.

In the cut-off region, the input frequency is much higher than the resonant frequency, so $\Omega^2 \gg 1$. If we ignore the other terms, we find that

$$2\alpha \sin(kd) - i\Omega^2 = 0.$$

This equation is satisfied when the real part of the wave number $k_r \approx \pi/d$. This result predicts that the wavelength gets no shorter than twice the tilt distance, and explains why k_r asymptotes to the same value independent of α . For a tilt distance $d = 71\mu\text{m}$, this estimate yields the value of 44.2, which is quite close to the simulation result of 49.5. This discrepancy is mostly attributed to the difference in the values of γ we used in the simulation and the approximation.

Finally, to zero the imaginary part, k_i , we have to simultaneously satisfy

$$(\Omega^2 - 1)k_r + 2\Omega\rho/M(x) = 0 \quad \text{and} \quad 2\alpha \sin(k_r d) - \zeta\Omega = 0.$$

The first equation guarantees that the imaginary terms cancel out while the second is what is left to constrain the real terms. We can assume $\sin(k_r d) \approx \pi - k_r d$ if the peak occurs near the cut-off region and still ignore Ω^2 if it is not too close. In that case, we obtain

$$k_r = \frac{1}{1 + m\zeta/2\alpha} \frac{\pi}{d} \quad \text{and} \quad \Omega = \frac{m}{1 + m\zeta/2\alpha} \pi,$$

where $m = M(x)/2\rho d$, which is equal to 0.21 for our parameter values. For $\alpha = 0.1, 0.15,$ and 0.2 , these approximations yield values of $k_r = 36.5, 38.8,$ and 40.0 , and $\Omega = 0.55, 0.58,$ and 0.60 , respectively. The first two estimates for k_r are reasonably close to the simulation results of 30.9 and 34.9. However, the simulation diverged in the third case (i.e., when $\alpha = 0.2$).

V. DISCUSSION

As the OHC motility factor α changed, we observed radically different behavior outside the long-wave region. When α is zero (Fig. 3A), k_r drops near zero after the characteristic place whereas it stays almost unchanged in the active case (Fig. 3B). Thus, the wave speeds up apical to the peak position in the passive case, whereas it stays slow in the active case. For k_i , whereas the sign remains negative in the passive case, we observe positive values right before the peak location in the active case. It is these positive values

that produce large amplification of BM displacement in the active case.

We observed a bifurcation at $\alpha = 0.159$ (corresponding responses not shown in Fig. 2 and 3). Above this value, the BM response explodes (Fig. 2A and 3B). Further analytical work is required to understand the nature of this bifurcation. Our preliminary numerical simulations indicated that including the saturation of the OHC forces eliminates this instability; this modification to our linear model produced compression at high sound levels as well.

In conclusion, the present linear active model shows responses comparable to physiological data. Adding active OHC forces, exerted on the BM through its own cell body forwardly and through the PhP backwardly, to a passive 2D cochlear model greatly enhances amplification and frequency selectivity. These bi-directional, feed-forward and feed-backward, OHC forces cooperate to locally enhance BM motion when the wavelength is just right, acting like a spatial filter.

ACKNOWLEDGMENT

We would like to thank Dr. James C. Saunders for early discussion on the cochlear anatomy.

REFERENCES

- [1] W. E. Brownell, "Observation on a motile response in isolated hair cells," in *Mechanism of Hearing*, W. R. Webster and L. M. Aiken, Eds. Melbourne: Monash University Press, 1983, pp. 5-10.
- [2] C. D. Geisler, "A cochlear model using feedback from motile outer hair cells," *Hearing Research*, vol. 54, pp. 105-117, 1991.
- [3] A. Hubbard, "A traveling-wave amplifier of the cochlea," *Science*, vol. 259, 1993.
- [4] S. T. Neely, "A model of cochlear mechanics with outer hair cell motility," *J. Acoust. Soc. Am.*, vol. 94, pp. 137-146, 1993.
- [5] C. D. Geisler and S. Chunning, "A cochlear model using feed-forward outer-hair-cell forces," *Hearing Research*, vol. 86, pp. 132-146, 1995.
- [6] D. O. Lim and C. R. Steele, "A three-dimensional nonlinear active cochlear model analyzed by the WKB-numeric method," *Hearing Research*, vol. 170, pp. 190-205, 2002.
- [7] P. J. Kolston, M. A. Vierever, E. de Boer, and R. J. Diependaal, "Realistic mechanical tuning in a micromechanical cochlear model," *J. Acoust. Soc. Am.*, vol. 72, pp. 1441-1449, 1989.
- [8] C. R. Steele, G. Baker, T. J., and Z. D., "Electro-mechanical models of the outer hair cell," presented at Int. Symp. Biophysics of Hair Cell Sensory Systems, Singapore, 1993.
- [9] Y. Raphael, M. Lenoir, R. Wroblewski, and R. Pujol, "The sensory epithelium and its innervation in the mole rat cochlea," *J. Comp. Neurol.*, vol. 314, pp. 367-382, 1991.
- [10] R. V. Harrison and R. J. Mount, "The sensory epithelium of the normal and pathological cochlea," in *Physiology of the ear*, A. F. Jahn and J. Santos-Sacchi, Eds.: Thomson Learning, 2001, pp. 285-299.
- [11] K. E. Nilsen and I. J. Russel, "The spatial and temporal representation of a tone on the guinea pig basilar membrane," *PNAS Colloquium*, vol. 97, pp. 11751-11758, 2000.
- [12] L. Watts, "Cochlear Mechanics: Analysis and Analog VLSI." Pasadena: California Institute of Technology, 1993.

Corrections to “A Linear Cochlear Model with Active Bi-directional Coupling”

Bo Wen and Kwabena Boahen

Department of Bioengineering, University of Pennsylvania, PA, USA

This corrigendum applies to our paper titled “A Linear Cochlear Model with Active Bi-directional Coupling”, which was presented at the 25th Annual International Conference of the IEEE Engineering in Medicine and Biology Society in 2003 (EMBS’03). Only part B, Analytical Treatment, of Section IV—Simulation Results and Analysis, is affected; we rederived our results, to obtain more sound approximations. In addition, the value of BM stiffness per unit area $S(x)$ in Table I should be corrected as $5.0 \cdot 10^6 e^{-0.4x}$ g/(mm²s²), the actual parameter value that was used for all the simulations in the paper.

Analytical Treatment

We derive approximations that describe three characteristic features of the wavenumber locus, particularly for the active case (*i.e.*, $\alpha > 0$). First, why does it enter the first quadrant? Second, what is the asymptotic value of the real part? And, third, when is the imaginary part equal to zero? The first question sheds light on how active amplification arises. The second addresses why the wavelength remains short in the cut-off region, unlike the passive case. And the third reveals how the characteristic place depends on the model’s parameters.

Setting the forward to backward ratio $\gamma = 1$ ($\gamma = 0.3$ was used for above simulations) as an approximation, we obtain a dispersion relation of the form:

$$\frac{k \tanh(kh)}{1 + i\alpha S(x)k \tanh(kh) \sin(kd) / \rho \omega^2} = \frac{2\rho \omega^2}{S(x) + i\omega\beta(x) - \omega^2 M(x)}$$

In the short-wave region, $\tanh(kh) \approx 1$. Substituting this approximation yields

$$2\alpha k \sin(kd) - (\zeta\Omega + i(\Omega^2 - 1))k - 2i(\rho / M(x))\Omega^2 = 0,$$

where $\Omega = \omega / \omega_n$ and $\omega_n(x) = \sqrt{S(x) / M(x)}$. (Note: Omission of the second Ω^2 term led to errors that are corrected below.)

As $\sin(kd) \approx kd$ when $|kd| \ll 1$ near the base, we have

$$2\alpha dk^2 - (\zeta\Omega + i(\Omega^2 - 1))k - 2i(\rho / M(x))\Omega^2 = 0.$$

The input frequency is also much lower than ω_n , so $\Omega^2 \ll 1$. And we can assume that $\zeta\Omega \ll 1$ as well. Hence, we find that

$$k = (\sqrt{i16\alpha(\rho d / M(x))\Omega^2 - 1 - i} / 4\alpha d).$$

Ω increases as the wave propagates, due to the decrease in ω_n . Thus, the first term pushes the wavenumber into the first quadrant if $\alpha > 0$. Therefore, a non-zero OHC motility factor is the source of active amplification.

Near the apex, the input frequency is much higher than the resonant frequency, so $\Omega^2 \gg 1$. Therefore, we have

$$2\alpha \sin(kd) - i(1 + 2\rho / (kM(x)))\Omega^2 = 0.$$

This equation is satisfied when the real part of the wave number $k_r \approx \pi/d$ if $|k| \gg 2\rho / M(x)$. This result predicts that the wavelength gets no shorter than twice the tilt distance, and explains why k_r asymptotes to the same value independent of α . For a tilt distance $d = 71\mu\text{m}$, this estimate yields the value of 44.2, which is quite close to the simulation result of 49.5. This discrepancy is mostly attributed to the difference in the values of γ we used in the simulation and the approximation.

Finally, to zero the imaginary part, k_i , we have to simultaneously satisfy

$$(\Omega^2 - 1)k_r + 2\Omega^2 \rho / M(x) = 0 \quad \text{and} \quad 2\alpha \sin(k_r d) - \zeta\Omega = 0.$$

The first equation guarantees that the imaginary terms cancel out while the second is what is left to constrain the real terms. We can assume $\sin(k_r d) \approx \pi - k_r d$ if the peak occurs near the cut-off region and still ignore Ω^2 if it is not too close. In that case, given $\alpha \gg \zeta / 4\pi$, we obtain

$$k_r \approx \frac{\pi}{d} - \frac{\zeta}{2d\alpha} \frac{1}{\sqrt{1+1/m\pi}} \quad \text{and} \quad \Omega \approx \frac{1}{\sqrt{1+1/m\pi}},$$

where $m = M(x) / 2\rho d$, which is equal to 0.21 for our parameter values. The predicted value of Ω is 0.63, which is independent of α , a good approximation. For $\alpha = 0.1, 0.15,$ and 0.2 , these approximations yield values of $k_r = 35.4, 38.3,$ and 39.8 , respectively. The first two estimates for k_r are reasonably close to the simulation results of 30.9 and 34.9. However, the simulation diverged in the third case (*i.e.*, when $\alpha = 0.2$).